Factors Affecting the Properties of Friction Stir Welded Aluminum Lap Joints

Critical sheet interface was eliminated by either a second weld pass or refined tool dimensions, resulting in exceptional joint efficiency

BY L. CEDERQVIST AND A. P. REYNOLDS

ABSTRACT. Friction stir welding (FSW) is a solid-state joining process invented at The Welding Institute (TWI) in 1991. The ability to produce high-quality welds in high-strength aluminum alloys sets FSW apart from typical fusion welding techniques. The process has mainly been used for making butt joints in aluminum alloys. Development of FSW for use in lap joint production would expand the number of applications that could benefit from the technique.

In this study, an extensive investigation was carried out on FSW lap joints, including interface morphology and mechanical properties. Two materials, Alclad 2024-T3 and Al 7075-T6, sheet materials commonly used in the aerospace industry, were joined. Welding variables included welding speed, rotational speed and, of particular importance, tool dimensions.

Examination of metallographic cross sections and failure locations showed a critical sheet interface present in all welds. Consequently, a second weld pass was added to eliminate the critical sheet interface. Results indicated FSW lap joints may, on the basis of strength, potentially replace other joining processes like resistance spot welding and riveting.

Introduction

Friction Stir Welding

Friction stir welding (FSW) is a solid-state thermo-mechanical joining process, where the actual mechanism of weld formation is most nearly described as a combination of *in-situ* extrusion combined with forging. To produce a full-penetration groove weld in a butt joint, the bottom of the tool must be close to the bottom of the workpiece (which must be supported on the back side). In order to make a lap joint, the bottom of the tool must only extend through the bottom of the top sheet and into the bottom sheet, creating a metallic bond between the two sheets. Schematic drawings of the lap joint welding process are shown in Fig. 1 (Ref. 1).

Figure 1 also provides information regarding the terminology used to describe friction stir welds. Due to the tool rotation, friction stir welds are not symmetric about the weld centerline. The side of the weld on which the rotational velocity of the tool has the same direction as the welding velocity is designated the advancing side of the weld. The side of the weld on which the two velocities have opposite direction is designated the retreating side of the weld.

Friction stir welding of aluminum alloys results in the characteristic microstructure described in several previous studies (Refs. 2, 3). In lap joint welding, the movement of material within the weld was more important than the microstructure, due to the interface present between the sheets. The general features of the movement of material in butt joint welding have also been described in previous papers (Refs. 4, 5). Of particular interest was the transport of material from the retreating side to the advancing side at the top surface of the weld. This material transport resulted in vertical transport of material about the longitudinal axis of the weld. This same vertical transport occurred in lap joint welding (Ref. 6). If the vertical motion of material took place outside of the pin diameter, the unbonded sheet interface material could also be transported vertically, affecting the strength of the lap weld, as will be shown later.

Figures 2A–D show the vertical transport in several FSW butt joints of 8.1-mm-thick Al 2195-T8 produced using different welding parameters. The marker insert technique used to elucidate the vertical flow has been described in previous publications (Ref. 5). The figure illustrates the positions of inserted markers prior to welding (2A) and after welding using different weld pitches (tool advance per revolution, 2B-D). The positions of the markers are projected onto the transverse plane of the weld and the plate thickness direction is vertical in the figures. In each of Figs. 2A–D, the retreating side of the weld is on the left and the advancing is on the right. It can be seen a lower ratio of welding speed to rotational speed (resulting in a "hot" weld) caused more vertical transport on the retreating side (compare Fig. 2B with 2C), while a higher welding speed (resulting in a "colder weld") caused less vertical transport on the retreating side (compare Fig. 2C with 2D). The amount of vertical

KEY WORDS

Friction Stir Welding
Lap Joints
Aluminum Alloys
2024 and 7075
Solid State

L. CEDERQVIST and A. P. REYNOLDS are research assistant and professor, respectively, in the Mechanical Engineering Department at the University of South Carolina, Columbia, S.C.

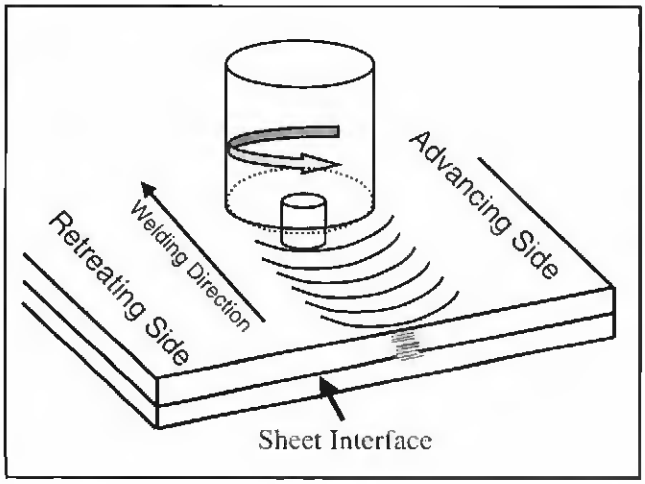

Fig. 1 — Schematic of friction stir welding process and definitions of FSW terminology.

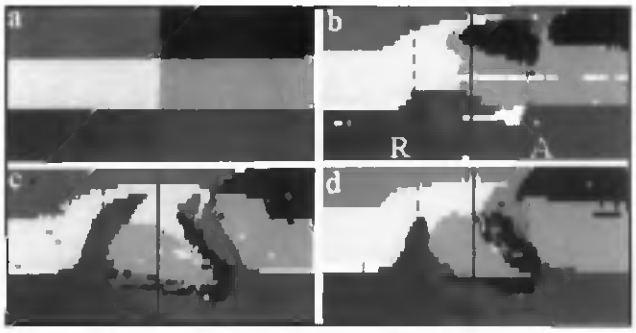

Fig. 2 — Vertical transport in an 8.1-mm-thick Al 2195-T8 FSW butt joint using embedded marker material (Al 5454-H32). The solid and dashed lines denote the centerline and pin diameter, respectively. Marker positions are projected onto a transverse cross-section plane. The retreating side is on the left and the advancing on the right in every case. A — Positions of markers (transverse to the welding direction) before welding; B — positions of markers after welding for a weld using medium welding speed and medium tool rotation speed; C — positions of markers after welding for a weld using medium welding speed and high tool rotation speed; D — positions of markers after welding for welds using high welding speed and high tool rotation speed.

transport can be judged by the height in the weld achieved by the lowest retreating side marker. In 2B, the marker does not reach the mid-plane of the weld. In 2C, the marker extends over more than two-thirds of the weld height and in Fig. 2D, it is between one-half and two-thirds of the weld height. The weld pitch is highest for 2B and lowest for 2C with 2D intermediate.

In a different study of material flow in friction stir welds, Colligan (Ref. 6) used a steel shot tracer technique to visualize material flow in 6.4-mm-thick Al 7075-T6. Results indicated, for example, that material closer to the bottom of the pin on the retreating side translated less upward than material closer to the top of the sheet. For reasons to be discussed in another section, optimization of the overlap shear strength of FSW lap joints required management of the vertical transport of material during welding operations.

Competitive Joining Processes

Riveting is currently the primary method of joining aerospace structures and has been used in aircraft fabrication since the 1920s (Ref. 7). The maximum overlap shear strength found in MIL-HDBK-5 (Ref. 8) was 10.3 kN using Al-alloy solid rivets (one-piece fasteners), 9.2 kN using blind fasteners, and 14.4 kN using Ti-6Al-4V swaged collar fasteners.

Resistance spot welding (RSW) is a process of welding by use of force and current. RSW is currently the joining method of choice in the automobile industry (steel sheet primarily) for economic reasons (Ref. 9). However, in an ongoing effort to reduce weight, aluminum alloy use in the automobile industry has expanded tremendously. The maximum overlap shear strength found in MIL-HDBK-5 was 7.4 and 15.4 kN for single- and multiple-row spot weld joints, respectively.

Experimental Procedure

Materials

Alclad 2024-T3 and bare 7075-T6 were used, respectively, as the top and bottom sheet of the lap joints. The nominal composition in weight percent (major alloying additions) of the 2024 is 4.4% Cu-1.5% Mg-0.6% Mn and balance aluminum. The nominal composition of 7075 is 1.6% Cu-2.5% Mg-0.23% Cr-5.6% Zn and balance aluminum. Sheet thickness for 2024-T3 and 7075-T6 are 2.29 mm (0.090 in.), while the cladding of 2024-T3 sheets is 0.06 mm thick on both sides. The ultimate tensile strength (UTS) of 2024-T3 base metal is 475 MPa; the UTS of 7075-T6 base metal is 595 MPa.

Welding Procedures

All FSW lap joints were made on a 15-hp vertical milling machine. Both top and bottom sheets were 610 mm long and 127 mm wide and were positioned as shown in Fig. 1. Sheets were degreased prior to welding using a household cleaner. No mechanical means of oxide removal were employed. However, scale on the sheets was very light.

Table 1 lists the welding parameters used for all welds, as well as the failure load and failure location(s) in overlap shear testing. The welding speed (WS) ranged from 2.3 to 5.6 mm/s and the rotational speed (RS) of the tool ranged from 300 to 983 rpm. Seven different WS-RS combinations were used for the 25 welds produced in this study.

Nine different tool configurations were used. Pertinent tool dimensions are detailed in Table 2 and defined in Fig. 3. Due to relatively short pin lengths and no fixed rotational direction, the tools were made without threads. Tool-to-workpiece angle was maintained at 2.5 deg for all welds. A shoulder plunge of 0.5 x (shoulder diameter) x sin (2.5 deg) was used for all welds. This shoulder plunge resulted in shoulder contact with the base plate at the tool centerline perpendicular to the welding direction.

Welds were made in either one pass (single pass) or two passes (double pass). When double-pass welds were made, both passes were made with the same tool and welding parameters. However, the tool rotation was reversed for the second pass and the tool was moved over toward the advancing side of the first weld, while welding direction and top sheet were maintained constant. As a result, the advancing sides of both passes were adjacent to each other and contained within the weld nugget, while the retreating sides of both passes were on the periphery of the weld nugget. The separation distance, designated SE (column 6 in Table 1), refers to the distance between the centerlines of the two weld passes in double-pass welds.

Overlap Shear Testing

Lap joints may be loaded primarily ei-

Table 1 — Welding Parameter and Overlap Shear Test Data

Weld No. Loaded	Tool No.	WS (mm/s)	RS (rpm)	SP/DP	SE (mm)	F Load (kN) R (R1) Loaded	F Locations R (R1) Loaded	F Load (kN) A (R2) Loaded	F Locations A (R
1	1	2.3	495	SP	—	7.0	A,B	14.0	A, T, t.n.
2	2	2.3	495	SP	—	n/a	n/a	8.3	A, T
3	3	2.3	495	SP	—	8.0	t.n.	9.4	t.n.
4	4	2.3	495	SP	—	n/a	n/a	5.6	A, T
5	5	2.3	495	SP	—	8.5	A, B	12.2	t.n.
6	6	2.3	495	SP	—	10.9	A, B	14.0	A, T
7	9	2.3	300	SP	—	21.4	A, B	15.6	A, T
8	1	2.3	495	DP	3.8	14.4	R1, T	15.1	R2, T
9	6	2.3	495	DP	3.8	17.8	R1, T	17.7	R2, T
10	6	2.3	495	DP	6.4	18.3	R1, T	19.6	R2, T R1, B
11	6	3.3	495	DP	3.8	16.7	R1, T	18.6	R2, T R1, B
12	6	3.3	638	DP	3.8	17.7	R1, T	14.9	R1, B
13	6	3.3	638	DP	6.4	16.7	R1, T	17.1	R1, B
14	6	3.3	638	DP	8.9	18.0	R1,T	20.3	R2, T R1, B
15	6	4.2	983	DP	5.1	16.1	R1, T	16.7	R2, T R1, B
16	6	4.2	833	DP	5.1	15.6	R1, T	17.0	R2, T
17	5	3.3	495	DP	5.8	15.7	R1, T	18.1	R2, T
18	5	5.6	495	DP	5.8	17.7	R1, T	17.9	R1, B
19	7	2.3	300	DP	8.9	19.6	R1, T	21.4	R1,B
20	7	2.3	495	DP	8.9	16.4	R1, T	16.6	R2, T
21	8	2.3	300	DP	8.9	20.0	R1, T	23.0	R2, T HAZ
22	8	3.3	495	DP	8.9	20.9	R1, T	23.8	R1, B
23	9	2.3	300	DP	8.9	22.8	R1, T	22.6	R2, T R1, B
24	9	3.3	495	DP	8.9	23.2	R1, T HAZ	23.3	R2, T R1, B
25	9	4.2	833	DP	8.9	20.9	R1, T	22.4	R2, T

WS = welding speed; RS = rotational speed; SP = single pass; DP = double pass; SE = separation distance; F = failure; t.n. = through nugget

ther in shear or by peel. In this study, the strength of lap joints loaded nominally in overlap shear is examined. In an ideal lap shear test (no bending), the tensile stress in the top and bottom sheets progressively decreases from a maximum at the loaded end to zero at the unloaded end. Figure 4 shows the theoretical tensile stress distribution in a lap joint with no sheet interface present and no bending. In a real lap shear test, particularly if no guides are used, additional tensile stresses will be generated at the bottom of the loaded side of the top sheet and at the top of the loaded side of the bottom sheet. Corresponding compression stress components will be generated on the opposite sides of the sheets. These stresses arise due to bending of the sheets around axes perpendicular to the loading direction and passing through points near the edges of the metallic-bonded interface (Ref. 10). These bending stresses increase the test's severity and may be deleterious when the lap joint interface has components normal to the nominal shear-loading direction (that is when the unbonded-interface direction is in the sheet-thickness direction).

Due to the asymmetric nature of FSW, a lap joint can be loaded with the advancing side loaded (experiencing maximum stress according to Fig. 4) on the top sheet (Fig. 5B) or with the retreating side loaded on the top sheet (Fig. 5A). Double-pass welds can also be loaded in two ways according to Figs. 5C–D. The shapes of the sheet interfaces in Figs. 5A–D are general representations for FSW lap joints produced in this study. It can be seen how the sheet interface on the retreating side has moved upward (interface pull up), while the advancing side can have both upward and downward movement. The sheet interface on the retreating side is gently curved, while on the advancing side, the interface generally exhibits abrupt changes in direction. Because of the stress distribution described in Fig. 4 and due to the bending stresses present, the critical locations in Fig. 5A will be in the top sheet on the retreating (R) side and in the bottom sheet on the advancing (A) side.

The time between welding and shear testing was typically 120 h so that post-weld natural aging would not vary appreciably from weld to weld. All overlap shear tests were performed on a 100-kN MTS testing machine at a constant crosshead displacement rate of $2.5 \cdot 10^{-2}$ mm/s. The maximum (failure) load and failure location were recorded for each specimen. In this study, specimens were designated according to which side of the top sheet (2024-T3) was loaded (experiences maximum load): A for advancing and R for retreating in the case of single-pass welds, and R1 or R2 (meaning the retreating side of pass 1 or pass 2) in the case of double-pass welds (Fig. 5A–D). Relative positions of the sheets during welding (Fig. 1) were such that specimens could be cut out of the welded sheets in both possible loading conditions. Two specimens for each weld and each loading condition were tested and the failure loads averaged. All specimens tested were 25.4 mm wide (see Fig. 6 for dimensions of test specimens). The failure load for a 25.4-mm-wide specimen of the Al-clad 2024-T3 base metal sheet was 27.6 kN, which was used to calculate the joint efficiency of the welds.

Table 2 — Tool Dimensions

Tool No.	Pin Length (mm)	Pin Diameter (mm)	Shoulder Diameter (mm)
1	4.0	5.1	12.7
2	4.0	4.4	12.7
3	3.0	5.1	12.7
4	3.0	4.4	12.7
5	4.0	5.9	12.7
6	3.0	4.8	15.7
7	3.6	9.7	25.4
8	3.3	9.7	25.4
9	3.0	9.7	25.4

Optical Microscopy

Optical microscopy was used to study transverse cross sections of the welds. Standard metallographic polishing procedures were used with Keller's reagent

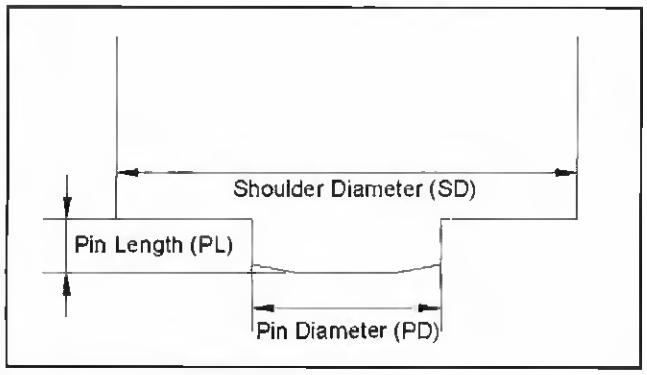

Fig. 3 — Definitions of tool dimensions.

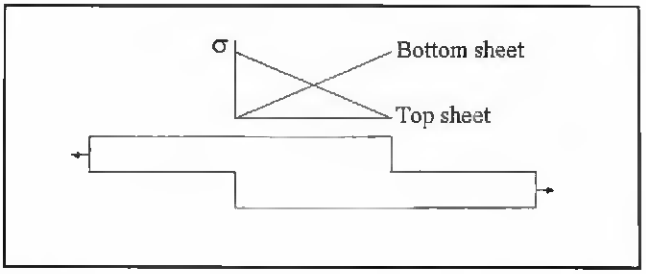

Fig. 4 — Theoretical stress distribution in a lap joint with no sheet interface present. In an actual unguided lap shear test, the specimen will also experience substantial bending stresses, as described in the text.

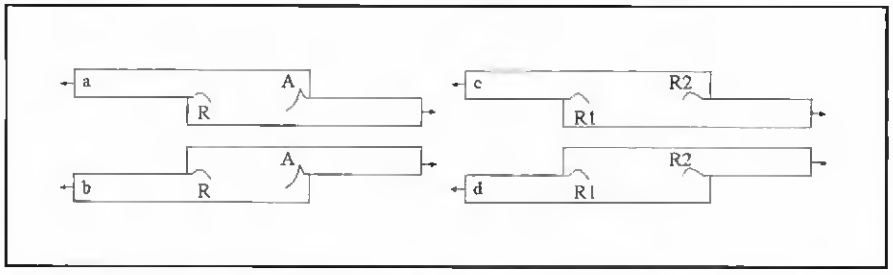

Fig. 5 — General schematic of FSW lap joints (including typical interface features) and definitions of possible configurations for overlap shear testing. Arrows indicate loading directions. A — R-loaded, single-pass weld in lap joint; B — A-loaded, single-pass weld in lap joint; C — R1-loaded, double-pass weld in a lap joint; D — R2-loaded, double-pass weld in a lap joint.

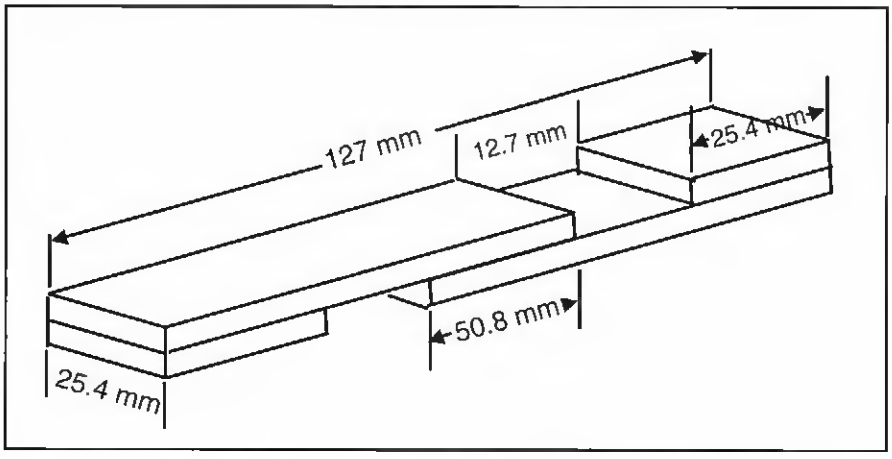

Fig. 6 — Overlap shear specimen. All dimensions are in mm.

to prepare the specimens. In addition, it was concluded the shape and amount of upward or downward translation of the sheet interface was an important parameter. Therefore, a scale was used to measure how much of the original sheet thickness was left to carry the load after welding. On the basis of these measurements, a new parameter — effective sheet thickness (EST) — was introduced and defined according to Figs. 7A and D. The EST is the minimum sheet thickness determined by measuring the smallest distance between any unbonded interface and the top of the top sheet or bottom of the bottom sheet.

Hardness Measurements

One single-pass (No. 7) and one double-pass (No. 23) weld made with the same tool and welding parameters were sectioned and polished so the hardness could be measured using a Vickers hardness tester with a load of 200 g. Hardness measurements were performed to reveal possible changes due to the second weld pass. The middle of both the top and the bottom sheets were tested throughout the cross section with 0.5-mm spacing between data points.

Results

Overlap Shear Testing

The failure load and failure location from overlap shear testing for all of the welds are shown in Table 1.

Failure locations (columns 8 and 10) are designated with a weld side (A, R, R1, or R2) and a sheet (either top, T, or bottom, B); t.n. indicates through-nugget failure. The failure load for single-pass welds (not including weld No. 7) ranged from 5.6 to 14.0 kN (avg. 9.6 kN). Welds loaded on the top sheet, retreating side (R loaded) averaged 8.6 kN, while the top sheet advancing side-loaded (A-loaded) specimens for the same welds averaged 12.4 kN. For the R-loaded single-pass specimens, 80% failed on the advancing side, bottom sheet and 20% failed through the nugget (through-nugget failure). For the A-loaded single-pass specimens, 64% failed at the advancing side, top sheet, and 36% failed through the nugget. In other words, no retreating side failures were observed in single-pass welds. As a result, there was a need to eliminate the critical advancing side and prevent through-nugget failure. Accordingly, the double-pass welding technique was developed, since it would eliminate

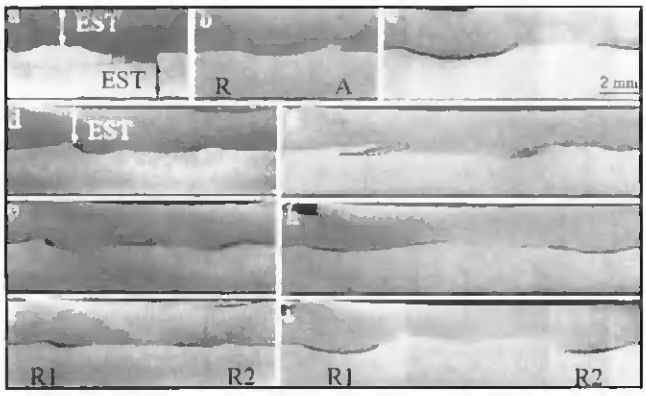

Fig. 7 — Metallographic cross sections of FSW lap joints (transverse to welding direction). The top sheet is Alclad 2024, and the bottom sheet is 7075 in all cases. For single-pass welds (A–C), the advancing side is on the right. For double-pass welds, R1 is on the left. A — Single-pass weld No. 1, showing the locations of the minima in the EST (effective sheet thickness) on the advancing and retreating sides. The difference in interface shape (advancing vs. retreating) may also be observed. B — Single-pass weld No. 3, identical to weld No. 1 except for reduced pin length. C — Single-pass weld No. 7, identical to No. 3 except for increased (2X) shoulder and pin diameters. Note the relatively flat interface. D — Double-pass weld No. 9 showing the location of the minimum EST on the R1 side. E — Double-pass weld No. 10 identical to No. 9 except for wider separation distance resulting in unbonded interface in the center of the weld. Note the similarities between the interface shapes in D and E. F — Double-pass weld No. 11. Higher welding speed relative to D and E results in a flatter interface (increased EST). G — The interface shape is comparatively flat. H — Double-pass weld No. 21 illustrating the effect of reduced pin length relative to G. The interface shape is comparatively flat. I — Double-pass weld No. 23 showing interface push down resulting from use of a pin length less than that used in weld No. 21.

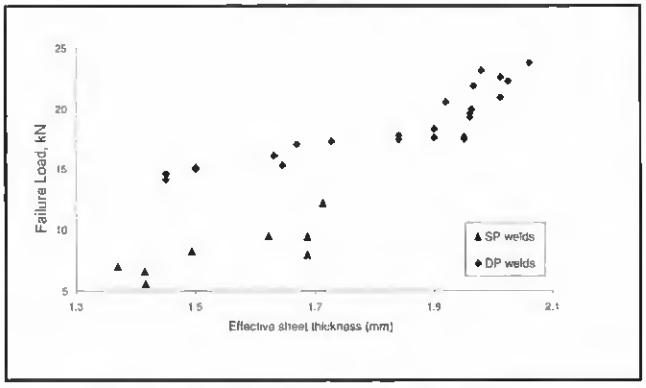

Fig. 8 — Graph of failure load vs. effective sheet thickness.

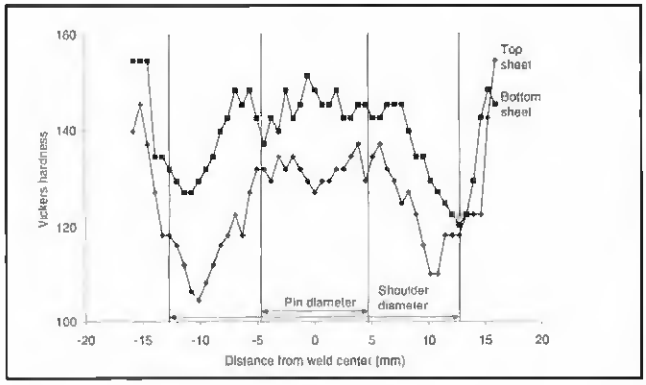

Fig. 9 — Graph of Vickers hardness distribution (transverse to welding direction) for a single-pass weld.

both the advancing side and make the weld nugget wider, hence preventing through-nugget failure.

The failure load for double-pass welds ranged from 14.4 to 23.8 kN (avg. 18.7 kN). R1-loaded specimens averaged 18.2 kN, while the R2-loaded specimens averaged 19.2 kN. For the R1-loaded double-pass specimens, 100% failed on the R1 side, top sheet. For the R2-loaded double-pass specimens, 56% failed on the R2 side, top sheet, and 44% failed on the R1 side, bottom sheet.

The failure load for the single-pass weld No. 7 was 21.4 kN for the R-loaded specimens and 15.6 kN for the A-loaded specimens. All weld No. 7 specimens failed on the advancing side either top or bottom sheet. Weld No. 7 will be discussed further in another section.

Optical Microscopy

Figures 7A–I show metallographic cross sections of several single- and double-pass welds. Figures 7A–C are single-pass welds with the advancing side on the right and the retreating on the left. The difference between the advancing and retreating side interfaces can be readily observed in the first single-pass weld — Fig. 7A. For Fig. 7B, all parameters were kept the same as for Fig. 7A except the pin length was reduced by 25%. It can be seen this lessened the amount of pull up on the retreating side and caused pull up, instead of pull down, on the advancing side. Figure 7C has the same pin length as Fig. 7B but twice the pin and shoulder diameter. As a result, a larger weld nugget and a smoother shape of the interface on the advancing side were produced.

Considering the double-pass welds shown in Figs. 7D and 7E, all weld parameters are the same except that Fig. 7E has a larger separation distance between the first and second passes (greater than the pin diameter), resulting in an unbonded interface in the middle of the weld nugget. For Fig. 7F, welding speed was increased relative to Figs. 7D and E resulting in less pull up of both retreating sides (R1 and R2) compared to Fig. 7D. This is consistent with the trends in vertical flow of material shown in Fig. 2. The effect of pin length on interface shape of the retreating side can once more be observed in Figs. 7G, H and I, which used pin lengths of 3.6, 3.3, and 3.0 mm, respectively. The longest pin caused interface pull up, while the middle length pin resulted in a flatter interface, and the shortest pin caused interface pull down. This correlates well with the work presented by Colligan (Ref. 4).

Figure 8 is a graph of the failure load as a function of effective sheet thickness (EST) for all single- and double-pass welds that did not exhibit through-nugget failures. It is apparent that increasing EST results in increased failure loads for both single- and double-pass welds. Comparing single- and double-pass welds having the same EST, double-pass welds exhibit higher failure loads.

Hardness Measurements

Figures 9 and 10 show results from the hardness measurements of a single-pass weld (No. 7) and double-pass weld (No. 23), respectively. The vertical lines indicate the position of the tool shoulder and pin during welding. For the single-pass weld, hardness varied between 105 and 154 and 120 and 154 for the top and bottom sheet, respectively. For the double-pass weld, hardness varied between 105 and 151 and 118 and 168 for the top and bottom sheet, respectively. The base metal hardness was 155 for the top sheet (2024-T3) and 170 for the bottom sheet (7075-T6).

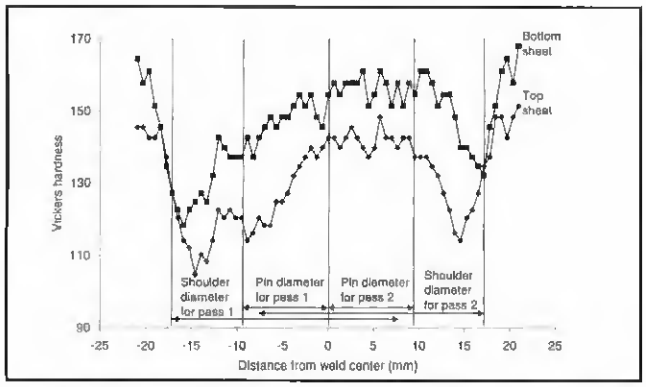

Fig. 10 — Graph of Vickers hardness distribution (transverse to welding direction) for a double-pass weld.

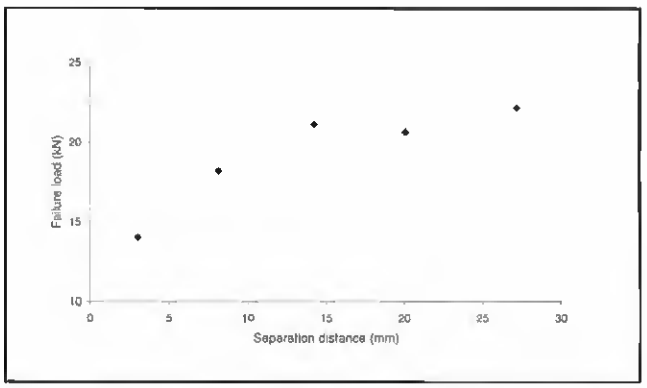

Fig. 11 — Graph of failure load vs. separation distance for double-pass welds.

Discussion of Results

Effective Sheet Thickness

As mentioned earlier, from examination of metallographic cross sections of the single-pass and double-pass welds, it was supposed the effective sheet thickness, (defined in Figs. 7A and D), can be related to the strength of both single- and double-pass welds. Figure 8 confirms this hypothesis. The reason a single-pass weld with the same EST as a double-pass weld has lower strength is likely due to the sharpness or minimum radius of curvature of the interface (higher stress concentration) on the advancing side of the single-pass weld compared to either retreating side in the double-pass welds.

Figure 8 indicates the strongest welds are obtained using welding parameters and tool dimensions that result in as little interface pull up of the retreating side as possible (indicated by the maximum EST). Two important findings were made. First, higher welding speed or lower rotational speed (both resulting in a "colder" weld) result in less pull up on the retreating side (compare Figs. 7D and F). This observation agrees with the paper by Seidel and Reynolds (Ref. 5) that found a colder weld has less vertical mixing of material, especially on the retreating side — Figs. 2A–D. However, it has been shown in other aluminum alloys (*e.g.*, Ref. 11) that if weld parameters result in too cold a weld, poor metallic bonding between the top and bottom sheets may result. Second, shorter pin length results in less pull up of the retreating side — Figs. 7G, H, and I. On the retreating side, material flows less upward near the bottom of the pin than at the middle of the pin, which results in less pull up of a sheet interface that is closer to the bottom of the pin than to the middle. In fact, pull down of the sheet interface was achieved for the shortest pin (Fig. 7I), and for the combination of alloys used in the joint studied. This is beneficial because it causes thinning of the stronger sheet (7075). In summary, improved interface shape is obtained when the faying surface between the two sheets is near the bottom of the pin.

Separation Distance

Table 1 shows a larger separation distance (the distance between the centers of the first and second weld passes) in double-pass welds usually gives a stronger weld, although there is a "crack" or unbonded interface left in the middle of the weld if the separation distance is greater than the pin diameter. The likely explanation for this is the longer weld nugget inhibits bending of the loaded specimen (Ref. 10), reducing the bending-induced tensile stress at the critical interface between metallic bonded and unbonded material at the faying surface of the lap weld. A separate investigation was made (Ref. 12) to further understand the influence of weld nugget length on weld strength. The result (failure loads for R1- and R2-loaded specimens averaged) can be seen in Fig. 11. The failure load increases with increasing separation distance up to approximately 15 mm. Beyond 15 mm, separation distance has only a small effect on strength. For SP welds, weld nugget length equals pin diameter, while for double-pass welds, weld nugget length equals pin diameter plus separation distance.

A- vs. R-Loaded Single-Pass Welds

For single-pass welds, A-loaded specimens are significantly stronger than R-loaded specimens because on the advancing side, the interface pull down is generally more severe than the interface pull up, causing greater reduction in EST on the bottom sheet (7075-T6) than on the top sheet (2024-T3). As seen in Fig. 7A, there is undetectable pull up but critical pull down of the advancing side, which causes A-loaded specimens to be twice as strong as the R-loaded specimens (which failed on the advancing side, bottom sheet) for weld No. 1.

Weld No. 7 (Fig. 7C) is a single-pass weld made with a tool (No. 9) modified to produce interface pull down of the retreating side. However, the tool also produced a desirable interface on the advancing side. Unlike other single-pass welds, the interface on the advancing side had no sharp corners. In addition, the R-loaded specimens exhibited exceptional strength, due to the interface pull up on the advancing side.

R1- vs. R2-Loaded Double-Pass Welds

For double-pass welds, the R2-loaded specimens were marginally stronger than the R1-loaded specimens. Comparing failure locations for double-pass welds, R2-loaded specimens failed 44% on the R1 side, bottom sheet, while R1-loaded specimens never failed on the R2 side, bottom sheet (always on the R1 top sheet). This was probably the result of using weaker material (2024) on the top sheet and the effect of the second pass on the R1 hardness distribution, which will be discussed below.

For two of the strongest welds, No. 21, R2-loaded (23.0 kN, 83% joint efficiency), and No. 24, R1-loaded (23.2 kN, 84% joint efficiency), the failure location was in the top sheet close to the edge of the shoulder. This location is the heat-affected zone (HAZ), in terms of microstructural zones (Ref. 2). At this location, no vertical mixing occurs, so the failure load is unaffected by the sheet interface. The failure loads and locations

are similar to results of FSW butt joints in Al 2024-T3. For example, in Ref. 13, Reynolds, *et al.*, report a joint efficiency of 83% was achieved and the failure occurred in the HAZ of the retreating side.

Hardness Measurements

For the single-pass weld (Fig. 9), there was minimum hardness in both the advancing and retreating side HAZs. The hardness of the nugget was higher than in the HAZ, but lower than the base metal values. No substantial differences could be seen between the advancing and retreating sides. For the double-pass weld (Fig. 10), the hardness profile was similar to that of the single-pass weld except the gradient in hardness between the HAZ minimum and the local peak in the nugget was much more gradual on the R1 side than on the R2 side. It appears the additional heat treatment imposed by the second weld pass caused softening of the R1 nugget. This phenomenon could explain why R1-loaded specimens tended to be weaker than the corresponding R2-loaded specimens. Comparison of the minimum hardness values for the single- and double-pass welds indicates almost no difference; only the distribution of hardness is modified by the second weld pass. This indicates the HAZ regions of both the single- and double-pass welds may be in a minimum hardness condition for the two alloys.

Conclusions

Testing results and analysis conducted on FSW lap joints have provided the following conclusions and salient observations:

1) A maximum joint efficiency of 86% (23.8 kN of max. 27.6 kN) was achieved for the FSW lap joints in this study. This is comparable to joint efficiencies reached for FSW butt joints of the same materials. For single-pass welds, a maximum joint efficiency of 78% was achieved, which is at least 60% stronger than comparable riveted and RSW lap joints.

2) For double-pass welds, the second weld pass does not cause a reduction in minimum hardness. However, hardness distribution is modified compared to that of the single-pass welds.

3) In the presence of sufficient bonded interface width to prevent through-nugget shear, two critical factors influencing overlap shear strength of FSW lap joints are EST and sheet interface shape. Sheet interface should not have any sharp corners (stress concentrations) or defects (cavities). For double-pass welds, separation distance should be less than, or equal to, the pin diameter to prevent the formation of unbonded interface within the weld.

4) A "cold" weld (low rotational speed and/or high welding speed) causes less vertical mixing of the retreating side. Likewise, a shorter pin (as long as the pin length exceeds the thickness of the top sheet) causes less vertical mixing of the sheet interface, hence maximizing the EST.

5) In addition to providing sufficient area to prevent failure by through-nugget shear, a wider weld nugget is beneficial because it decreases the amount of bending in a nominally shear loading configuration. Therefore, a tool with a large pin diameter may be favorable for welds loaded in overlap shear.

6) If a single-pass weld is produced, the welding direction should be chosen so the joint is A loaded, because the advancing side usually exhibits undetectable pull up, but critical pull down. However, if tool dimensions are used that cause pull down of the retreating side, an R-loaded joint may exhibit higher strength (*i.e.*, weld No. 7). Likewise, if a double-pass weld is produced, a R2-loaded joint will usually exhibit higher strength.

Acknowledgments

This research was performed with support from NASA Langley Research Center, Rob Hafley, technical monitor. Special thanks to Dan Wilhelm for helping with weld production, tool refinements, and overlap shear testing.

References

1. *http://www.ewi.org/matjoin/resistance/frictionstir.html*

2. Rhodes, C. G., Mahoney, M. W., and Bingel, W. H. 1997. Effects of friction stir welding on microstructure of 7075 aluminum. *Scripta Materialia* 36(1): 69–75.

3. Strangwood, M., Berry, J. E., Cleugh, D. P., Leonard, A. J., and Threadgill, P. L. 1999. Characterization of the thermo-mechanical effects on microstructural development in friction stir welded age hardening aluminum-based alloys. *1st International Symposium on Friction Stir Welding*, Thousand Oaks, Calif.

4. Colligan, K. 1999. Material flow behavior during friction stir welding of aluminum. *Welding Journal* 78(7): 229-s to 237-s.

5. Seidel, T. U., and Reynolds, A. P. Visualization of the Material Flow in AA2195 friction stir welds using a marker insert technique. Accepted by *Metallurgical Transactions, A.*

6. Cederqvist, L., and Reynolds, A. P. 2000. Properties of friction stir welded aluminum lap joints. *Proceedings of the 2nd International Symposium on Friction Stir Welding*. Gothenburg, Sweden.

7. Irving, B. 1997. Why aren't airplanes welded? *Welding Journal* 76(1): 31–41.

8. MIL-HDBK-5H. 1998. Metallic materials and elements for aerospace vehicle structures. 8–27,37,108,148.

9. Thornton, P. H., Krause, A. R., and Davies, R. G. 1996. The aluminum spot weld. *Welding Journal* 75(3): 101-s to 108-s.

10. Schijve, J. 1972. Some elementary calculations on secondary bending in simple lap joints. NLR TR 72036.

11. Dracup, B. J., Arbegast, W. J. 1999. Friction stir welding as a rivet replacement technology. *SAE Conference*. Nashville, Tenn.

12. Reynolds, A. P., Cederqvist, L. 2000. Secondary parameters influencing strength in FSW lap joints. Unpublished work.

13. Reynolds, A. P., Lockwood, W. D., Seidel, T. U. 2000. Processing-property correlation in friction stir welds. *Materials Science Forum* 331–337: 1719–1724.